Communication

Communication: Remarkable electrophilicity of the oxalic acid monomer: An anion photoelectron spectroscopy and theoretical study

Angela Buonaugurio, Jacob Graham, Allyson Buytendyk, Kit H. Bowen, Matthew R. Ryder, Zibo G. Keolopile, Maciej Haranczyk, and Maciej Gutowski

Citation: The Journal of Chemical Physics **140**, 221103 (2014); doi: 10.1063/1.4882655
View online: http://dx.doi.org/10.1063/1.4882655
View Table of Contents: http://scitation.aip.org/content/aip/journal/jcp/140/22?ver=pdfcov
Published by the AIP Publishing

Communication: Remarkable electrophilicity of the oxalic acid monomer: An anion photoelectron spectroscopy and theoretical study

Angela Buonaugurio,[1] Jacob Graham,[1] Allyson Buytendyk,[1] Kit H. Bowen,[1,a)]
Matthew R. Ryder,[2,b)] Zibo G. Keolopile,[2,3,a)] Maciej Haranczyk,[4] and Maciej Gutowski[2,a)]
[1]*Department of Chemistry, Johns Hopkins University, Baltimore, Maryland 21218, USA*
[2]*Institute of Chemical Sciences, School of Engineering and Physical Sciences, Heriot-Watt University, Edinburgh, Scotland, EH14 4AS, United Kingdom*
[3]*Department of Physics, University of Botswana, Private Bag 0022, Gaborone, Botswana*
[4]*Computational Research Division, Lawrence Berkeley National Laboratory, One Cyclotron Road, MS 50F-1650, Berkeley, California 94720, USA*

(Received 23 April 2014; accepted 29 May 2014; published online 13 June 2014)

Our experimental and computational results demonstrate an unusual electrophilicity of oxalic acid, the simplest dicarboxylic acid. The monomer is characterized by an adiabatic electron affinity and electron vertical detachment energy of 0.72 and 1.08 eV (±0.05 eV), respectively. The electrophilicity results primarily from the bonding carbon-carbon interaction in the singly occupied molecular orbital of the anion, but it is further enhanced by intramolecular hydrogen bonds. The well-resolved structure in the photoelectron spectrum is reproduced theoretically, based on Franck-Condon factors for the vibronic anion → neutral transitions. © *2014 AIP Publishing LLC*. [http://dx.doi.org/10.1063/1.4882655]

I. INTRODUCTION

Stable, closed-shell organic molecules with heteroatoms, such as monocarboxylic acids (formic, acetic), nucleic acid bases, and amino acids, usually do not support bound valence anionic states in the neighbourhood of the optimal geometry of the neutral species.[1] These molecules still support metastable (resonant) anionic states, with finite lifetimes and energies higher than the energy of the neutral,[2–4] but they are not able to permanently bind an excess electron in a valence orbital. The electrophilicity of these molecules is typically enhanced upon specific geometric distortions, including tautomerizations.[5,6] In consequence, valence anionic states are frequently characterized by positive values of electron vertical detachment energies (VDE), while adiabatic electron affinities (AEA) of the corresponding neutrals might remain negative (CO_2[5]), approach zero (canonical uracil[7]), or settle at positive values (unconventional tautomers of guanine[8,9] and adenine,[10] nucleotides[11,12]). Here, we report a significant electrophilicity of the oxalic acid (OA) monomer. It is the simplest dicarboxylic acid, see Figure 1, which may be viewed as a product of condensation of two formic acid molecules (with the release of H_2). Let us reemphasize that the formic acid monomer does not support a bound valence anionic state.

The neutral OA molecule can exist in three conformational forms (structures **1–3** in Figure 1); it also has a local minimum for a "rare tautomer" (structure **4**). These minimum energy structures differ in the extent of intramolecular hydrogen bonding; this phenomenon attracted attention of many experimental[13–19] and computational[20–25] groups. Indeed, the gas phase structure of the neutral OA monomer has been studied by electron diffraction,[13] infrared and Raman spectroscopy,[13,14] matrix-isolation,[15–17] UV absorption,[18] microwave spectroscopy,[19] and theoretically at various levels of theory.[20–25] Here, we report a photoelectron spectrum (PES) of the OA monomer anion, which reveals a significant electrophilicity of the neutral; where the main spectral features extend from 0.5 to 2.5 eV (Figure 2). Our computational results provide an interpretation of this well-resolved photoelectron spectrum.

II. COMPUTATIONAL METHODS

The minimum energy structures and harmonic frequencies for **1–5** of OA and OA^- were determined at the coupled-cluster single double (CCSD) level of theory and single-point energies were determined at the coupled-cluster single double triple (CCSD(T)) level.[26] Initial calculations were performed with the aug-cc-pVDZ[27] (ADZ) basis set. For the most stable neutral and anionic structure **3**, the calculations were repeated with the aug-cc-pVTZ[27] (ATZ) basis set. The electronic structure calculations have been carried out with the Gaussian 09[28] and MOLPRO[29] codes. Molecular structures and orbitals were plotted with the GMolden program.[30]

The Franck-Condon (FC) factors, i.e., the squares of overlap integrals between vibrational wave functions for the anionic and neutral OA, were calculated in harmonic approximation with molecular structures and Hessians determined at the CCSD/ATZ level. Both geometrical equilibrium parameters as well as curvatures are affected by excess electron attachment and the resulting FC factors may contribute to vibrational structure in the photoelectron spectrum. The

a)Authors to whom correspondence should be addressed. Electronic addresses: m.gutowski@hw.ac.uk; kbowen@jhu.edu; and keolopilezg@mopipi.ub.bw
b)Current address: Department of Engineering Science, University of Oxford, Parks Road, Oxford OX1 3PJ, United Kingdom. matthew.ryder@eng.ox.ac.uk

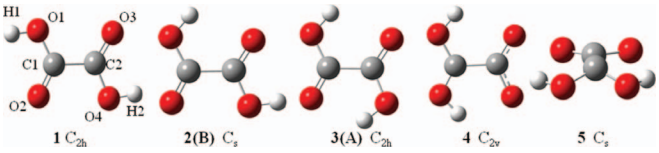

FIG. 1. Conformers and tautomers of the oxalic acid monomer. The naming scheme for atoms is shown for **1**.

polyatomic FC factors were calculated using the recursion relations of Doktorov.[31,32] The simulations were performed for different temperatures of the anionic beam (25 K < T < 300 K). The energy of the 0-0 transition was determined from the CCSD(T)/ATZ electronic energies and the CCSD/ATZ zero-point harmonic frequencies. The intensity for the 0-0 transition was normalized to 1 and all other intensities were scaled accordingly. The calculated FC factors were convoluted with Lorentzian line shapes (full width at half maximum = 218 cm^{-1}) and the simulated spectrum is presented in Figure 2.

III. EXPERIMENTAL DETAILS

Negative ion photoelectron spectroscopy is conducted by crossing a mass-selected beam of parent negative ions with a fixed-frequency photon beam and energy-analyzing the resultant photodetached electrons. This process is governed by the energy conserving relationship $h\nu = EKE + EBE$, where $h\nu$ is the photon energy, EKE is the measured electron kinetic energy, and EBE is the electron binding energy. OA anions were generated in a biased (−500 V) supersonic expansion nozzle-ion source, in which the OA sample was heated between 80 and 100 °C and co-expanded with approximately several atmospheres of argon gas through a 10 μm diameter nozzle. Low energy electrons were injected directly into the expanding jet by a hot and even more negatively biased thoriated iridium filament, in the presence of a weak external magnetic field where the microplasma was formed. The anions were then extracted and transported by an ion optics series through a 90° magnetic sector, mass spectrometer with a typical mass resolution of ∼400. The mass-selected OA anion beam was then crossed with an intracavity run argon ion laser beam. The resultant photodetached electrons were energy-analyzed in a hemispherical electron energy analyzer with a resolution of ∼30 meV. The photoelectron spectrum reported here was recorded with 2.540 eV photons (488 nm) and calibrated against the well-known photoelectron spectrum of the O^- anion.[33]

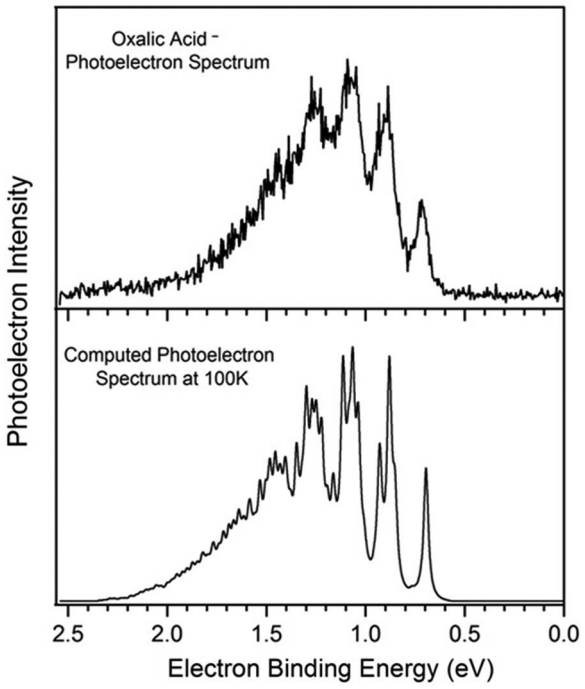

FIG. 2. (Upper trace) Photoelectron spectrum of OA^- recorded with 2.540 eV photons. (Lower trace) Computed spectrum based on the CCSD(T)/ATZ electronic energies and CCSD/ATZ geometries and Hessians.

IV. RESULTS

The landscape of the potential energy surface for neutral and anionic OA is summarized in Figure 3. The conformer **3** is stabilized by two intramolecular hydrogen bonds, thus the stability decreases along the series **3** → **2** → **1**, which agrees with previous findings.[20] The structures of the minima and transitions states TS1–TS3 for the neutral and anion are detailed in Tables S1 and S2 of the supplementary material.[34] The CCSD(T) barriers determined at the CCSD transition states separating neutral conformers are large enough (0.602 eV for **3** → **2** and 0.519 eV for **2** → **1**) to support a few vibrational states for **2** and **1**. The "rare tautomer" **4**, which may be viewed as a product of intramolecular proton transfer, is a local minimum on the potential energy surface of the neutral, but it is less stable than **3** by 1.010 eV and the barrier for **4** → **3** is only 0.020 eV.

The OA monomer supports a bound valence anionic state: all anionic minima (**1**–**3**, and **5**) are more stable than the most stable neutral **3** by a few tenths of an eV. **3** is the most stable anionic conformer (Figure 3). The barriers separating

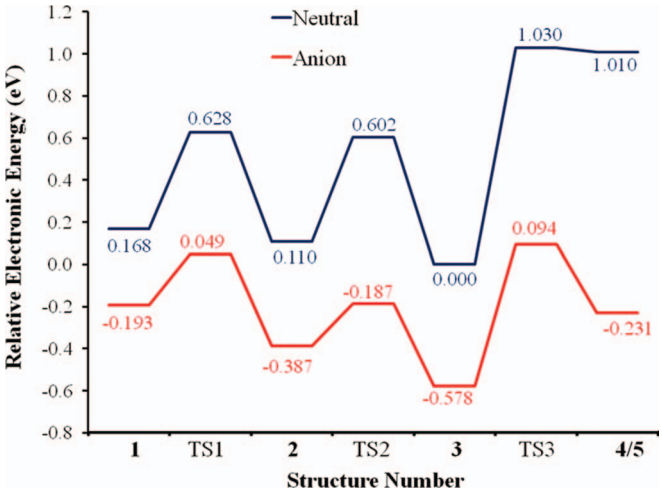

FIG. 3. Energetics of stationary points (minima and transition states) on the potential energy surface of the neutral and anionic monomer of oxalic acid, where the zero of energy is set to the energy of the neutral **3**.

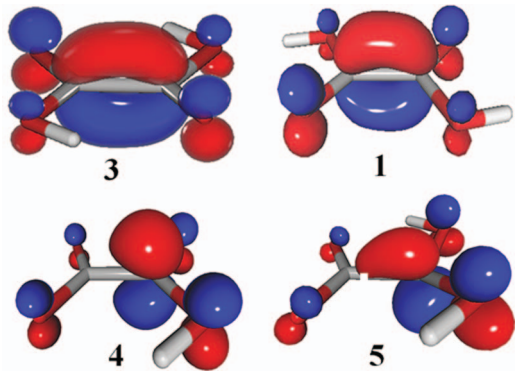

FIG. 4. The SOMO of anionic OA structures plotted with a contour value of 0.1 a.u.

conformers **1–3** are smaller for the valence anion than for the neutral. The tautomer **4** is strongly stabilized by the excess electron attachment. The molecular framework for the anion lowers symmetry from C_{2v} (structure **4**, with an imaginary frequency for a b_1 mode) to C_s (structure **5**) and the CCSD(T) barrier for **5** → **3** becomes 0.325 eV, thus one order of magnitude larger than the barrier **4** → **3** for the neutral. Thus, the anion **5** may be sufficiently long-lived to be observed in experimental conditions.

Which factors contribute to the stability of valence anions of the OA monomer? The singly occupied molecular orbital (SOMO) is of π symmetry (Figure 4). The SOMO is characterized by a bonding C-C interaction and antibonding C-O interactions, which is clearly illustrated for the C_{2h} structures **3** and **1**. A similar pattern holds for **4** and **5**, though the carbon atoms are not equivalent due to lower symmetries. We believe that the unique electrophilicity of OA results primarily from the proximity of the carboxylic groups, which allows for the bonding C-C interaction in the SOMO.

There are also secondary factors that contribute to the stability of valence anions of OA. The CCSD(T) values of VDE (Figure 5(a)) increase from **1** to **3** demonstrating that intramolecular hydrogen bonding stabilizes the anion. An even greater increase of VDE is brought by intramolecular proton transfer as the value of VDE increases by 0.605 eV from **3** to **4**. Finally, a buckling of the molecular framework further increases the value of VDE (**4** → **5**) by 0.591 eV.

The buckling of molecular frameworks upon binding an excess electron on a π^* orbital is a common phenomenon in valence anions of nucleic acid bases.[6] In the case of the most stable valence anion of OA, **3**, the framework remains unbuckled and the C_{2h} symmetry is maintained. Notice, however, that the buckling mode of b_g symmetry is softer by 201.7 cm^{-1} for the anion than for the neutral (Table I). It requires the intramolecular proton transfer (**3** → **4**) to change the sign of the curvature of the buckling mode. Upon intramolecular proton transfer the unpaired electron becomes localized on the $C(OH)_2$ fragment (bottom of Figure 4) and the C atom forms an apex of the buckled structure (Figure 1). The stationary point, **4**, is a transition state for the valence anion and the b_1 mode has an imaginary frequency of $\sim 300i$ cm^{-1}. This mode morphs into a′ symmetry mode of **5** with a frequency of $\sim$800 cm^{-1}.

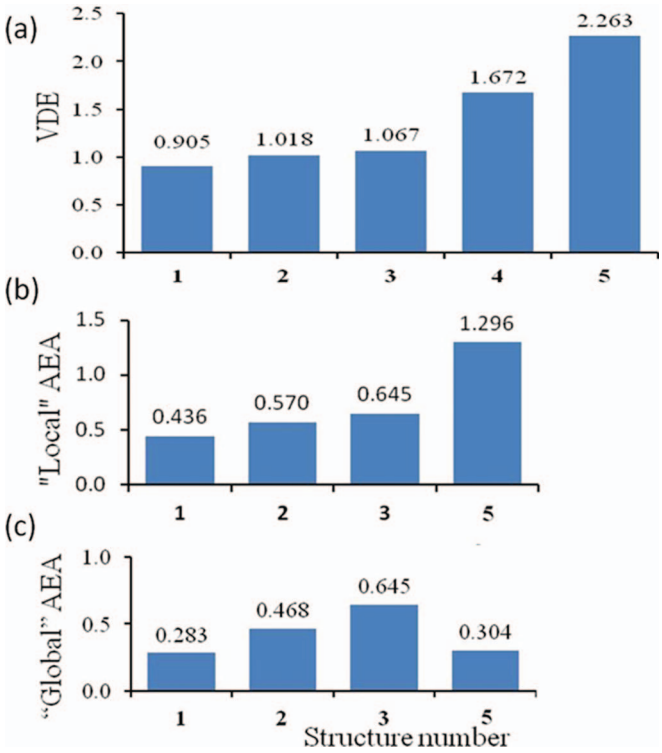

FIG. 5. Excess electron binding energies (eV) for the oxalic acid monomer. (a) The VDE values are reported. The AEA values are reported with respect to (b) the corresponding neutral ("Local" AEA), and (c) the most stable neutral **3** ("Global" AEA).

The electron binding energies (VDE, AEA) are summarized in Figure 5. The AEA values are corrected for the energies of zero-point vibrations and are reported with respect to the corresponding neutral ("Local" AEA, Figure 5(b)), and the most stable neutral **3** ("Global" AEA, Figure 5(c)). For

TABLE I. Nature of vibrational modes and harmonic frequencies, calculated at the CCSD/ATZ level for structure **3**. The "buckling" mode in bold, the modes contributing primarily to the vibronic structure reported in Figure 2 are in italic.

			Frequency (cm^{-1})	
Mode	Symmetry	Nature	Neutral	Anion
1	$\mathbf{a_u}$	C–C rotation	122.7	190.0
2	$\mathbf{b_u}$	C–C–O bend	269.4	255.0
3	$\mathbf{a_u}$	Buckling	481.5	403.5
4	$\mathbf{a_g}$	C–C stretch	418.6	411.8
5	$\mathbf{a_g}$	C–C–O bend	572.7	603.5
6	$\mathbf{b_u}$	C–C–O bend	683.3	612.6
7	$\mathbf{b_g}$	C–O(H) rotation	686.5	615.9
8	$\mathbf{a_u}$	C–O(H) rotation	691.2	633.3
9	$\mathbf{b_g}$	**Buckling**	**855.5**	**653.8**
10	$\mathbf{a_g}$	C–C stretch	848.1	836.3
11	$\mathbf{b_u}$	C–O(H) stretch	1233.5	1082.5
12	$\boldsymbol{a_g}$	*C–O–H bend*	*1262.1*	*1278.5*
13	$\mathbf{b_u}$	C–O–H bend	1368.4	1322.6
14	$\boldsymbol{a_g}$	*C–O(H) stretch*	*1490.3*	*1424.2*
15	$\mathbf{b_u}$	C=O stretch	1894.8	1628.2
16	$\boldsymbol{a_g}$	*C=O stretch*	*1884.5*	*1780.1*
17	$\mathbf{b_u}$	O–H stretch	3737.4	3732.6
18	$\mathbf{a_g}$	O–H stretch	3733.6	3735.9

each structure, we report significant differences between the VDE and "Local" AEA values, which must be associated with geometric distortions, such as changes of bond lengths and angles, upon binding an excess electron. These will be critical for the discussion of the PES spectrum of OA^-. Notice that the "Global" AEA values (Figure 5(c)) remain positive for all structures.

The experimental PES spectrum of OA^- is presented in black in Figure 2 (upper trace). It covers from ∼0.5 to 2.5 eV, with well-defined peaks at 0.72, 0.90, 1.08, 1.27, and 1.40 eV (±0.05 eV). In view of the fact that the anionic minimum **3** is more stable than other minima by more than 0.2 eV (Figure 3), we focused our attention on FC factors for the structure **3** anion → neutral vibronic transitions, and we assumed that contributions from other anionic structures to the experimental PES spectrum are less probable. Two observations support this assumption: (i) the position of the highest peak in the experimental spectrum (1.08 ± 0.05 eV) coincides with the calculated value of VDE for **3** of 1.13 eV, and (ii) the position of the first peak in the spectrum at 0.72 ± 0.05 eV coincides with the calculated value of AEA for **3** of 0.70 eV.

The calculated FC factors and signal intensities are presented in Table S3 of the supplementary material[34] and the resulting computed spectrum is presented in Figure 2 (lower trace). The best match with the experimental spectrum was found for T = 100 K. A very good agreement between the computed and experimental spectra suggests that the experimental anionic beam is indeed dominated by the most stable anionic structure **3**. Notice, however, a nonzero photoelectron intensity at approximately 2.2–2.3 eV, where the computed spectrum has no intensity. This weak feature might result from a small fraction of structure **5** in the anionic beam, with the calculated VDE of 2.26 eV (Figure 5(a)).

Further analysis of harmonic frequencies (Table I) and geometric parameters (Table II) of the neutral and anion of **3** is needed to understand the origin of the vibronic structure reported in Figure 2 and Table S3 of the supplementary material.[34] The C–C bond contracts and the C–O bonds elongate upon excess electron attachment. These are significant distortions, exceeding 0.05 Å. In addition, the C–C=O and C–O–H angles expand and contract, respectively, by 4° and 5°. The geometric distortion from the anion to the neutral can be accomplished by displacements along the fully symmetric modes 10, 12, 14, and 16. These are C–O or C–C stretching modes with the exception of 12, which is a C–O–H bending mode (Table I). The geometric changes are consistent with the nature of the SOMO in the anion, which is bonding in the C–C region and antibonding in the C–O regions (Figure 4). The C–O stretching modes 14 and 16 are strongly red-shifted upon an excess electron attachment by 66 and 104 cm^{-1}, respectively (Table I). Finally, perusal of the data from Table S3 of the supplementary material[34] confirms that the largest FC factors are associated with the 0-0 transition at 0.72 eV, and vibrational excitations involving the modes 12, 14, and 16, which are responsible for the developments of PES peaks at 0.90, 1.08, 1.27, and 1.40 eV (±0.05 eV).

TABLE II. Geometric parameters for the neutral and anionic structure **3** at the CCSD/ATZ level.

Parameter	Neutral	Anion
C1–C2	1.538	1.422
C1–O1	1.321	1.382
C1=O2	1.200	1.253
O1–H1	0.970	0.969
H1…O4	2.118	2.099
C2–C1–O1	113.58	113.94
C2–C1=O2	121.20	125.41
C1–O1–H1	107.19	102.70

V. SUMMARY

The oxalic acid monomer displays electrophilicity uncharacteristic for most simple organic molecules. It supports a bound valence anion in the neighbourhood of the global C_{2h} minimum of the neutral. The bound valence anion is characterized by an AEA of 0.72 eV and a VDE of 1.08 eV (±0.05 eV). The unique electrophilicity of OA results primarily from the proximity of the carboxylic groups, which allows for the bonding C-C interaction in the SOMO of the anion. The intramolecular hydrogen bonding also contributes to the overall stability of the anion. The PES of OA^- can be modelled based on the calculated AEA value of OA and the intensities of vibronic transitions given by Franck-Condon factors.

ACKNOWLEDGMENTS

This material is based, in part, upon experimental work supported by the (U.S.) National Science Foundation under Grant No. CHE-1360692 (K.H.B.). Z.G.K. was supported by the fellowship from the University of Botswana. This research was supported in part (to M.H.) by the U.S. Department of Energy under Contract No. DE-AC02-05CH11231. This research used resources of the National Energy Research Scientific Computing Center, which is supported by the Office of Science of the U.S. Department of Energy under Contract No. DE-AC02-05CH11231.

[1]NIST webbook, Standard Reference Database 69, see http://webbook.nist.gov/chemistry/, May 2012.
[2]M. Allan, Phys. Rev. Lett. **98**, 123201 (2007).
[3]K. Aflatooni, G. A. Gallup, and P. D. Burrow, J. Phys. Chem. A **102**, 6205 (1998).
[4]A. M. Scheer, P. Mozejko, G. A. Gallup, and P. D. Burrow, J. Chem. Phys. **126**, 174301 (2007).
[5]G. L. Gutsev, R. J. Bartlett, and R. N. Compton, J. Chem. Phys. **108**, 6756 (1998).
[6]X. Li, K. H. Bowen, M. Haranczyk, R. A. Bachorz, K. Mazurkiewicz, J. Rak, and M. Gutowski, J. Chem. Phys. **127**, 174309 (2007).
[7]R. A. Bachorz, W. Klopper, and M. Gutowski, J. Chem. Phys. **126**, 085101 (2007).
[8]M. Haranczyk and M. Gutowski, Angew. Chem., Int. Ed. **44**, 6585 (2005).
[9]M. Haranczyk, M. Gutowski, X. Li, and K. H. Bowen, J. Phys. Chem. B **111**, 14073 (2007).
[10]M. Haranczyk, M. Gutowski, X. Li, and K. H. Bowen, Proc. Natl. Acad. Sci. U.S.A. **104**, 4804 (2007).
[11]S. T. Stokes, A. Grubisic, X. Li, Y. J. Ko, and K. H. Bowen, J. Chem. Phys. **128**, 044314 (2008).
[12]M. Kobylecka, J. Gu, J. Rak, and J. Leszczynski, J. Chem. Phys. **128**, 044315 (2008).

[13]Z. Nahlovsk, B. Nahlovsk, and T. G. Strand, Acta Chem. Scand. **24**, 2617 (1970).
[14]B. C. Stace and C. Oralratm, J. Mol. Struct. **18**, 339 (1973).
[15]R. L. Redington and T. E. Redington, J. Mol. Struct. **48**, 165 (1978).
[16]J. Nieminen, M. Rasanen, and J. Murto, J. Phys. Chem. **96**, 5303 (1992).
[17]E. M. S. Macoas, R. Fausto, M. Pettersson, L. Khriachtchev, and M. Rasanen, J. Phys. Chem. A **104**, 6956 (2000).
[18]R. A. Back, Can. J. Chem. **62**, 1414 (1984).
[19]P. D. Godfrey, M. J. Mirabella, and R. D. Brown, J. Phys. Chem. A **104**, 258 (2000).
[20]C. Chen and S. F. Shyu, Int. J. Quantum Chem. **76**, 541 (2000).
[21]C. Vanalsenoy, V. J. Klimkowski, and L. Schafer, J. Mol. Struct.: THEOCHEM **109**, 321 (1984).
[22]G. Raabe, Z. Naturforsch., A **57**, 961 (2002); see online at http://cat.inist.fr/?aModele=afficheN&cpsidt=14468456.
[23]A. Mohajeri and N. Shakerin, J. Mol. Struct.: THEOCHEM **711**, 167 (2004).
[24]J. G. Chang, H. T. Chen, S. C. Xu, and M. C. Lin, J. Phys. Chem. A **111**, 6789 (2007).
[25]G. Buemi, J. Phys. Org. Chem. **22**, 933 (2009).
[26]R. J. Bartlett and M. Musial, Rev. Mod. Phys. **79**, 291 (2007).
[27]R. A. Kendall, T. H. Dunning, and R. J. Harrison, J. Chem. Phys. **96**, 6796 (1992).
[28]M. J. Frisch, G. W. Trucks, H. B. Schlegel *et al.*, Gaussian 09, Revision A.1, Gaussian, Inc., Wallingford, CT, 2009.
[29]H.-J. Werner, P. J. Knowles, G. Knizia, F. R. Manby, M. Schütz *et al.*, MOLPRO, version 2010.1, a package of *ab initio* programs, 2010, see http://www.molpro.net.
[30]G. Schaftenaar and J. H. Noordik, J. Comput.-Aided Mol. Des. **14**, 123 (2000).
[31]E. V. Doktorov, I. A. Malkin, and V. I. Manko, J. Mol. Spectrosc. **56**, 1 (1975).
[32]D. S. Yang, M. Z. Zgierski, D. M. Rayner, P. A. Hackett, A. Martinez, D. R. Salahub, P. N. Roy, and T. Carrington, J. Chem. Phys. **103**, 5335 (1995).
[33]D. M. Neumark, K. R. Lykke, T. Andersen, and W. C. Lineberger, Phys. Rev. A **32**, 1890 (1985).
[34]See supplementary material at http://dx.doi.org/10.1063/1.4882655 for CCSD/ADZ structures for the neutral and anion of oxalic acid, conformers **1–5**. CCSD/ADZ structures of the neutral and anionic transition states **TS1–TS3** of oxalic acid. Franck-Condon factors and signal intensities for the anion → neutral vibronic transitions of the most stable conformer **3**.